TITLE: Giant African snail genomes provide insights into molluscan whole-genome duplication and aquatic-terrestrial transition

Conghui Liu[+], Yuwei Ren[+], Zaiyuan Li, Qi Hu, Lijuan Yin, Xi Qiao, Yan Zhang, Longsheng Xing, Yu Xi, Fan Jiang, Sen Wang, Cong Huang, Bo Liu, Hengchao Wang, Hangwei Liu, Fanghao Wan, Wanqiang Qian*, Wei Fan*

Guangdong Laboratory of Lingnan Modern Agriculture, Shenzhen ; Genome Analysis Laboratory of the Ministry of Agriculture and Rural Affairs; Agricultural Genomics Institute at Shenzhen, Chinese Academy of Agricultural Sciences, Shenzhen, 518120, China.

The authors with symbol "[+]" contributed equally: Conghui Liu, Yuwei Ren; the authors with symbol "*" represented corresponding authors: Wanqiang Qian, Wei Fan.

Email: qianwanqiang@caas.cn; fanwei@caas.cn.

Abstract

Whole-genome duplication (WGD) has been observed across a wide variety of eukaryotic groups, contributing to evolutionary diversity and environmental adaptability. Mollusks are the second largest group of animals, and are among the organisms that have successfully adapted to the nonmarine realm through aquatic-terrestrial (A-T) transition, and no comprehensive research on WGD has been reported in this group. To explore WGD and the A-T transition in Mollusca, we assembled a chromosome-level reference genome for the giant African snail *Achatina immaculata*, a global invasive species, and compared the genomes of two giant African snails (*A. immaculata* and *Achatina fulica*) to the other available mollusk genomes. The chromosome-level macrosynteny, colinearity blocks, Ks peak and Hox gene clusters collectively suggested the occurrence of a WGD event shared by *A. immaculata* and *A. fulica*. The estimated timing of this WGD event (~70 MYA) was close to the speciation age of the Sigmurethra-Orthurethra (within Stylommatophora) lineage and the Cretaceous-Tertiary (K-T) mass extinction, indicating that the WGD reported herein may have been a common event shared by all Sigmurethra-Orthurethra species and could have conferred ecological adaptability and genomic plasticity allowing the survival of the K-T extinction. Based on macrosynteny, we deduced an ancestral karyotype containing 8 conserved clusters for the Gastropoda-Bivalvia lineage. To reveal the mechanism of WGD in shaping adaptability to terrestrial ecosystems, we investigated gene families related to the

respiration, aestivation and immune defense of giant African snails. Several mucus-related gene families expanded early in the Stylommatophora lineage, functioning in water retention, immune defense and wound healing. The hemocyanins, PCK and FBP families were doubled and retained after WGD, enhancing the capacity for gas exchange and glucose homeostasis in aestivation. After the WGD, zinc metalloproteinase genes were highly tandemly duplicated to protect tissue against ROS damage. This evidence collectively suggests that although the WGD may not have been the direct driver of the A-T transition, it provided an important legacy for the terrestrial adaptation of the giant African snail.

Introduction

Whole-genome duplication (WGD) is proposed to be a key evolutionary event driving phenotypic complexity, functional novelty, and ecological adaptation [1,2]. With the progress of high-throughput sequencing technologies, almost all fundamental lineages of land plants have been characterized as having undergone WGD, while far fewer WGDs among animal lineages have been reported, especially in invertebrate [3,4]. Based on chromosome counts and genome size, WGD events have been speculated to have occurred in mollusks, the second largest animal group, which have survived major extinction events and become some of the most successful conquerors of marine, freshwater and terrestrial environments [5,6]. Giant African snails, a group of species within Achatinidae possessing unusually large body sizes, have evolved from

aquatic ancestors and achieved a pulmonate terrestriality through an aquatic-terrestrial (A-T) transition [7]. Because of their remarkable ecological adaptability, some members of the giant African snails are considered global invasive species, causing serious damage to agriculture and households [8]. The success of their colonization of terrestrial ecosystems and adaptation to diverse environments suggests that giant African snails possess advanced genetic plasticity and evolutionary novelties, although the key drivers and underlying mechanisms remain poorly understood.

In contrast to plants, only a few ancient WGDs have been well documented in animals, because polyploidy is usually an evolutionary dead end, resulting from associated meiotic difficulties [9,10]. In vertebrates, several ancient WGD events that occurred at the origin of vertebrates and teleost fishes have been proposed to have shaped genetic diversity and adaptive radiation [11,12]. In animals other than vertebrates, less conclusive evidence of ancient WGD events has been reported as there is a deficiency of continuous high-quality genome data. Nevertheless, there are several known cases of large-scale genome duplication in groups, such as rotifers, chelicerates and insects. The genome of bdelloid rotifers is tetraploid, and its scaffolds are rearranged during asexual reproduction [13]. A possible ancestral WGD in chelicerates has been identified in horseshoe crab and was dated to at least 135 million years ago (MYA) through the phylogenetic analysis of Hox genes [14], and subsequent surveys in chelicerates revealed that the spider and scorpion lineages underwent another separate WGD before 430 MYA [15]. Because of the fragmental assembly and uncertain accuracy of traditional analysis methods, the validation of

WGD in invertebrates remains controversial. Surprisingly, Li et al. reported 18 ancient WGDs during the evolution of insects in a recent paper, while another macrosyteny analysis in lepidopterans showed that the gene-tree-based and Ks-based detection of WGD adopted by Li are unreliable, and suggested that WGD events should be verified by chromosome-scale genome assembly and macrosynteny analysis [16,17].

Regarding the A-T transition, the conquest of land by organisms that evolved from aquatic ancestors represents one of the most astonishing events in the history of life on Earth [18]. The dramatic environmental changes from homogeneous water habitat to the heterogenous land environment brought about a significant revolution in species evolution, leading to radiation diversity and life complexity [19,20]. This step was achieved in multiple phyla independently via a set of adaptations such as water balance, air breathing, nitrogen excretion, neural-immune system interactions, and certain behaviors [21]. Within Mollusca, the clade Pulmonata includes several lineages that invaded the terrestrial zone and non-aquatic ecosystems, especially the Stylommatophora [22]. The giant African snail within Stylommatophora is a representative of the land snails that has also developed fundamental machinery and behaviors such as a pulmonate lung, complex immune system, mucus production, and aestivation, making it highly adapted to the terrestrial environment [22-24]. Several reports on amphibious species have shown that the expansion and positive selection of genes related to innate immunity, nitrogen excretion, hormonal regulation and pulmonary surfactants were closely connected to the A-T transition [25], although the

genomic features and evolutionary characteristics of terrestrial invertebrates are still poorly described. Studies of the giant African snail, a promising model for terrestrial mollusks, will facilitate the elucidation of invertebrate A-T transition.

Mollusca is the second largest animal phylum constituting 7% of living animals on Earth [26], and comprises numerous species of evolutionary and economic importance [27,28]. However, the available genomic resources for Mollusca are still quite insufficient in comparison with those for other large phyla such as Arthropoda and Nematoda [29,30]. The genomes of aquatic mollusks such as California sea hare [31], Pacific oyster [32], pearl oyster [33,34], owl limpet [35], California two-spot octopus [36], golden mussel [37], *Biomphalaria glabrata* [38], and golden apple snail [39] have been sequenced, whereas few terrestrial species in Mollusca have well-documented genomic information. Recently, the genomic data of the invasive land snail *A. fulica* were released, but without in-depth studies of related biological issues [40]. To address the genetic and evolutionary characteristics of terrestrial mollusks, we report the genome of another giant African snail with a larger body size and greater invasiveness (Fig. 1a, b and c) [41], and provide insights into the molluscan WGD, A-T transition, and invasion mechanisms, through comparative genomic analysis between the two giant African snails and other closely related mollusks.

Results

The *A. immaculata* genome provides a better assembly and annotation for giant African snails

We generated 200 Gb (121 ×) of PacBio SMRT raw reads with an average read length of 14 kb, and 145 Gb (82 ×) of Illumina HiSeq paired-end reads using DNA extracted from a single adult of *A. immaculata* (Supplementary Table 1). After quality filtering, 199 Gb (120 ×) of clean PacBio SMRT reads were corrected with Canu [42], assembled with wtdbg2 [43], and polished with pilon [44], resulting in an assembly of 563 raw contigs with a total length of 1,653 Mb and an N50 length of 3.80 Mb. Based on the Hi-C data, 1,648 Mb (99.7%) of final contigs were anchored and arranged into 31 linkage groups, each corresponding to a natural chromosome (Fig. 1d, Supplementary Fig. 1), where the longest was 111.19 Mb and the shortest 34.32 Mb. According to an estimated genome size of 1.75 Gb based on the distribution of the k-mer frequency [32] (Supplementary Fig. 2), ~95% of the *A. immaculata* genome was assembled. To further confirm the accuracy and completeness of the assembly, we mapped the Illumina reads to the assembled reference genome. Significantly, 99.11% of the genome-derived reads could be aligned to the reference genome with a coverage rate of 96.50%, suggesting no obvious bias in sequencing and assembly. The high-quality reference genome provides a good foundation for gene annotation.

Protein-coding genes were predicted in the reference genome by using EVM, integrating *de novo* prediction, transcriptome and homology data (Supplementary

Table 2). In total, 28,702 gene models were predicted as the reference gene set, with coding regions spanning ~39.1 Mb (2.37%) of the genome (Supplementary Table 3 and 4). The distribution of CDS length in *A. immaculata* was similar to that in closely related species (Supplementary Fig. 3 and 4). Overall, 87.5% of the reference genes were supported by transcriptome data, and 96.27% of the eukaryotic core genes from OrthoDB (http://www.orthodb.org/) were identified in the reference gene set by BUSCO. These results were comparable to those obtained from other published molluscan genomes (Supplementary Table 4). In the functional annotation, a total of 26,616 (92.73%) reference genes were annotated according to at least one functional database (Supplementary Fig. 5).

The quality of this assembly is much better than that of other molluscan genomes published thus far (Supplementary Table 4). In particular, the coverage rate and sequence continuity were greatly improved compared with the most recent published *A. fulica* genome. The estimated genome size was 2.12 Gb, and the *A. fulica* genome was assembled into 1.86 Gb. The coverage rate of the *A. immaculata* genome (95%) was 8% higher than that of *A. fulica* (87%). The N50 and N90 lengths of the *A. immaculata* contigs were increased by 5.3 times and 4.9 times, respectively. With better assembly quality, ~5000 additional gene models were annotated in *A. immaculata*, and the BUSCO rate was improved from 93% (*A. fulica*) to 96% (*A. immaculata*). The high quality of the assembly and annotation of *A. immaculata* provide a better resource for research on giant African snails.

Signs of adaptive evolution in giant African snails

To gain insights into the evolution of giant African snails (*A. immaculata* and *A. fulica*), a total of 292,034 reference genes from ten molluscan genomes (Fig. 2) were clustered into 17,949 orthologous groups (OGs) containing at least two genes each. Then, a phylogenetic tree was built based on 229 high-confidence single-copy orthologous genes with RAxML [45] and the divergence time was estimated using R8S [46]. The results showed that *A. immaculata* diverged from *A. fulica* 21 million years ago (MYA), from *B. glabrata* (Panpulmonata) 174 MYA, from *A. californica* (Euopisthobranchia) 205 MYA, and from *P. canaliculata* (Caenogastropoda) 416 MYA (Fig. 2a). Through CAFE analysis, we identified 2225 expanded OGs in giant African snails (both *A. immaculata* and *A. fulica*). The functions of these OGs are mainly related to signal transduction; the endocrine, immune and nervous systems; longevity regulation and reproduction (Supplementary Fig. 6). Additionally, 836 OGs were found exclusively in the lineage of giant African snails, which mainly functioned in neurohormonal regulation and mucus synthesis and included such as acetylcholine receptor, pannexin, tenascin, adrenocorticotropic hormone receptor, neuropeptide receptor, 5-hydroxytryptamine receptor, mucin, heparan sulfate glucosamine 3-O-sulfotransferase and proteophosphoglycan genes (Fig. 2b, Source Data file). This evidence suggests that the expanded and lineage-specific OGs may play important roles in the adaptation and invasion of giant African snails.

This high-quality genome assembly enables a comprehensive analysis of transposable elements (TEs), which play multiple roles in driving genome evolution

192 in eukaryotes [47]. In total, we identified 954 Mb of repetitive sequences in the
193 assembled *A. immaculata* genome and 1,366 Mb in *A. fulica* (Fig. 2c). Next, we
194 analyzed the divergence rate of each class of TE among the available molluscan
195 genomes. Notably, the TE class of DNA transposons showed a specific peak at a
196 divergence rate of 4~6% for four invasive species, *A. immaculata, A. fulica, P.*
197 *canaliculata* and *C. gigas* (Fig. 2d), indicating a recent explosion of DNA transposons.
198 We identified 9,291 genes in region that contained DNA transposons distributed
199 within the specific divergence peak. Based on KEGG annotation, these genes were
200 mainly enriched in signal transduction; the endocrine, immune and nervous systems
201 and reproduction (Supplementary Fig. 7). TEs are powerful facilitators of evolution
202 that generate the "evolutionary potential" to introduce small adaptive changes within
203 a lineage, and the importance of TEs in stress responses and adaptation has been
204 reported in numerous studies [48,49]. The recent explosion of DNA TEs in giant African
205 snails could have played important roles in promoting their potential plasticity in
206 stress adaptation.

207 **Whole genome duplication in the Sigmurethra-Orthurethra branch**

208 Whole-genome duplication (WGD) has rarely been reported in animals,
209 especially in invertebrates, although there is growing suspicions of paleopolyploidy in
210 mollusks based largely on genome sizes and chromosome counts [6]. With
211 chromosome-level assemblies, we searched for macrosynteny based on homologous
212 gene pairs among four molluscan genomes, from *A. immaculata, A. fulica, P.*

213 *canaliculata* and *P. fucata*. Our chromosome-level macrosynteny revealed a WGD
214 event shared by two giant African snails, *A. immaculata* and *A. fulica*. The 31
215 chromosomes of *A. immaculata* could be divided into 14 groups with the preservation
216 of correspondence (Fig. 3a, Supplementary Fig. 8), and the same situation was found
217 in *A. fulica* (Fig. 3b, Supplementary Fig. 8). In *A. immaculata*, 2092 homologous gene
218 pairs with mutual best BLASTP hits were located on the corresponding chromosomes,
219 and this number was 2364 for *A. fulica* (Supplementary Table 5). The comparison of
220 the giant African snails, *P. canaliculata* (n = 14) and *P. fucata* (n = 14) revealed that
221 the karyotype doubled in the lineage leading to giant African snails (Fig. 3c, d and e).
222 The chromosomes of *A. immaculata* and *A. fulica* showed a 1 to 1 corresponding
223 relationship (Fig. 3c, Supplementary Fig. 8), while most chromosomes from *P.*
224 *canaliculata* (Fig. 3d, Supplementary Fig. 8) and *P. fucata* (Fig. 3d, Supplementary
225 Fig. 8) shared macrosynteny with 2 corresponding chromosomes from giant African
226 snails. The colinearity blocks identified by MCScanX based on BLASTP hits in
227 corresponding chromosome groups, also suggested that WGD events had occurred in
228 two giant African snails (Supplementary Fig. 9 and 10). In the gene age distribution
229 plot of homologous gene pairs, a specific Ks peak shared by *A. immaculata* and *A.*
230 *fulica* was observed, which was consistent with WGD. The duplication of Hox gene
231 clusters was powerful clue leading to the discovery of ancient WGDs in vertebrates [50],
232 so we further compared the giant African snails' genomes to those with a single Hox
233 cluster and no evidence of WGD. Duplicated Hox gene clusters with specific
234 rearrangements were found in two giant African snail genomes. In conclusion, the

235 macrosynteny, colinearity blocks, Ks peak and Hox gene clusters collectively
236 suggested that a WGD event occurred before the speciation of giant African snails.

237 The timing of WGD events has been reported to show a significant correlation
238 with specific geological and global climatic change [51]. According to the gene age
239 distribution of homologous gene pairs and the divergce time of *B. glabrata* and giant
240 African snails (~174 MYA), we deduced that the timing of the WGD event was ~70
241 MYA. An earlier estimation suggested the occurrence of a WGD event at the
242 Sigmurethra-Orthurethra branch within Stylommatophora by comparison of
243 chromosome numbers among closely related mollusks [6]. The speciation age of the
244 Sigmurethra-Orthurethra branch was reported to be 65 MYA, which was largely in
245 consistent with our deduced timing, indicating that the WGD reported here was a
246 common event shared by all Sigmurethra and Orthurethra species. The timing of the
247 WGD of the Sigmurethra-Orthurethra branch was also close to Cretaceous-Tertiary
248 (K-T) mass extinction (~66 MYA), in which global climate change caused the
249 extinction of 60-70% of all plant and animal life, including most mollusks [52]. In plants,
250 the K-T mass extinction is considered a shared common causal factor in the
251 genome-wide doubling of diverse angiosperm lineages [53]. It has also been previously
252 suggested that polyploidization in animals is correlated with periods of unstable
253 environments [1]. The WGD of the Sigmurethra-Orthurethra branch is expected to have
254 provided ecological adaptability and genome plasticity and allowed these taxa to
255 survive the K-T mass extinction.

256 As the terrestrial area expanded during the K-T mass extinction due to

Maastrichtian sea-level regression [54], the WGD is expected to have promoted the adaptability of land snails to terrestrial ecosystems and speciation diversity. The functions of WGD-derived homologous gene pairs were significantly enriched in biological regulation, signal transduction, energy generation and the response to stimulus (Supplementary Fig. 11). These functions are closely related to terrestrial living, indicating that the retained WGD-associated genes increased the terrestrial ecological tolerance of giant African snails.

The chromosome-level assembly of *A. immaculata*, *A. fulica*, *P. canaliculata* and *P. fucata*, allowed us to infer karyotype evolution within the clade of Gastropoda-Bivalvia based on macrosynteny. Our results indicated a monoploid chromosome number of n=8 for the root of the Gastropoda-Bivalvia lineage. This deduced chromosome number was consistent with that of Patellogastropoda (n=8~9) [55], which has been reported to exhibit monophyly in the Gastropoda-Bivalvia lineage and to present preserved ancestral characters [56]. During subsequent speciation, 6 breaks in the lineages of Gastropoda (n=14) and *P. fucata* (n=14) were observed at different locations. In the Gastropoda clade, Stylommatophora possessed 17 chromosomes, with fusion of chr4 and chr13 of Gastropoda, and showed 4 breaks in chr5 ,chr6 ,chr7 and chr8 of Gastropoda, while *P. canaliculata* retained the monoploid chromosome karyotype of Gastropoda (n=14). The WGD in the lineage of the Sigmurethra-Orthurethra branch doubled the chromosome count (n=17+17). After WGD, three fusions (chr6-chr15, chr8-chr16 and chr10-chr17 of Stylommatophora) resulted in the 31 chromosomes of the Sigmurethra-Orthurethra branch (n=17+14)

(Fig. 4). In the lineage of *A. immaculata* and *A. fulica*, a chromosome number n = 31 has remained since their speciation in 21 MYA. The demonstration of chromosome duplications, fusions and breaks provides insights into the ancestral karyotype and the mechanism of karyotype evolution in Gastropoda-Bivalvia.

Expansion of hemocyanins and zinc metalloproteinases improves terrestrial respiratory function

The innovation of respiratory gas exchange is the signature of the aquatic-to-terrestrial transition, which was one of the most conspicuous evolutionary events to have occurred on Earth [57]. The evolution of the oxygen transportation system allowed land snails to utilize O_2 from air far more efficiently than aquatic mollusks [58]. Additionally, an advanced system is needed to eliminate the accompanying oxidative stress to maintain O_2 homeostasis. However, the underlying mechanisms of O_2 transport and antioxidation are less well understood.

O_2 transport in most members of Gastropoda and Cephalopoda is dependent on hemocyanin [59]. Based on orthologous and phylogenetic analysis, hemocyanin genes were observed in six species of Gastropoda and Cephalopoda, which was consistent with previous reports [59,60]. Notably, there are 4 hemocyanin genes in both *A. immaculata* and *A. fulica*, which is twice as many as in any other Gastropoda species (Fig. 5a). Moreover, the four homologous genes of *A. immaculata* and *A. fulica* are located on two chromosomes that derived from WGD, whereas those of other species without WGD were only located in one chromosome or scaffold (Fig. 5b,

Supplementary Fig. 12 and 13). Thus, the doubling of the hemocyanin gene number through WGD may have increased the O_2 transport ability of giant African snails to adapt to land living.

Reactive oxygen species (ROS) are generated during O_2 metabolism, and excessive ROS cause oxidative stress and trigger inflammation [61]. However, antioxidant enzymes protect the host from excess oxidative damage. Superoxide dismutase (SOD), acid phosphatase (AP) and glutathione S transferase (GST) genes were identified in giant African snails, with gene numbers comparable to those of other molluscan species (Supplementary Table 6). In addition to antioxidant enzymes, metalloproteinases have the ability to hydrolyze fibronectin to reduce the injuries caused by ROS [62,63]. The number of zinc metalloproteinase genes in both giant African snails was largely expanded, to 11 in *A.immaculata* and 9 in *A. fulica*, compared to only 1 or 2 in other species (Fig. 5c, Supplementary Fig. 14 and 15). Importantly, the zinc metalloproteinase genes of the two species were located in two syntenic clusters on homologous chromosomes, while no homologous genes were found on the corresponding duplicated chromosomes resulting from WGD. The finding that the same location pattern was shared by the two species indicates that these genes were tandemly duplicated after the WGD event but before the specification of *A.immaculata* and *A. fulica*. Furthermore, the expression levels of all zinc metalloproteinases in the hepatopancreas and blood were higher than those in other tissues, which was consistent with the importance of the antioxidative function of these two tissues. Therefore, the expansion of zinc metalloproteinases after WGD

might have played important roles in the defense of giant African snails against the damage resulting from oxidative stress and inflammation.

Glucose homeostasis and ureagenesis benefit survival in aestivation

Aestivation in land animals is a special long-term torpid state that occurs in response to the extreme conditions of summer, such as desiccation, high temperature and starvation [64]. Terrestrial mollusks originating from aquatic ancestors, developed estivation as a strategy for surviving drastic environmental changes on land. During aestivation, giant African snails seal their shell aperture with epiphragma, and their body remains within the solid shell for several months [24]. During this long period, these snails are isolated from feeding and excretion, but their blood sugar level and toxic nitrogenous waste are maintained within a normal range. However, how the snails regulate blood glucose homeostasis and eliminate toxins during aestivation is still poorly understood.

Without sugar intake during aestivation, blood glucose homeostasis is mainly achieved via the exploitation of endogenous resources and the reduction of energy expenditure [65]. Regarding endogenous resources, glycogen is used initially, after which some portion of the carbohydrate skeleton associated with protein metabolism is primarily employed to produce blood glucose through gluconeogenesis [65]. In this study, we analyzed the expression level changes of two rate-limiting gluconeogenic enzymes phosphoenolpyruvate carboxykinase (PCK, EC:4.1.1.32) and fructose-1,6 - bisphosphatase (FBP, EC:3.1.3.11). Both enzymes are encoded by two homologous

genes derived from WGD, and the expression level of one homologous gene is significantly increased in aestivation (negative binomial generalized log-linear model, $p < 0.01$; Supplementary Table 7 and 8), while the other displays relatively constant expression. On the other hand, the consumption of glucose through the tricarboxylic acid (TCA) cycle is minimized in aestivation [66]. Several important enzymes are involved in the TCA, such as citrate synthase (EC:2.3.3.1), and malate dehydrogenase (EC:1.1.1.37) (Fig. 6a) [67]. Citrate synthase is encoded by two homologous genes derived from WGD, where one of the homologous genes is significantly downregulated (negative binomial generalized log-linear model, $p < 0.01$; Supplementary Table 7 and 8), while the other gene remains stable. The gene encoding malate dehydrogenase also presented significantly downregulated expression. This evidence indicates that blood glucose homeostasis during aestivation is achieved via both the upregulation of gluconeogenesis and downregulation of the TCA cycle.

The oxidative deamination of amino acids generates toxic ammonium (NH_3, NH_4^+), which can cause immunosuppression and neurotoxic effects [68,69]. In a normal state, giant African snails mainly convert ammonium into uric acid and excrete it out of their body through the urine, while during aestivation, they convert ammonium into urea and store it in their body [24,70]. The accumulation of nontoxic urea during aestivation has been proposed to play a role in the detoxification of nitrogenous substances, the reduction of evaporative water loss, and the reutilization of nitrogen resources [65].In this study, we analyzed the expression profiles of three important

enzymes involved in the urea cycle, including carbamoyl phosphate synthetase (CPS, EC:6.3.5.5), argininosuccinate synthetase (ASS, EC:6.3.4.5), and arginase (EC:3.5.3.1) [71]. All of the genes encoding these enzymes were significantly upregulated in the aestivation group compared with the normal group (Fig. 6b), providing insight into to the mechanism of the transformation of ammonia into urea during the aestivation of giant African snails.

Expanded mucus-related gene families reinforce immune defense

Molluscan immune defense has drawn increasing attention because of its economic and evolutionary importance [5,72]. As one of the most successful colonizers of terrestrial environments within Mollusca, giant African snails are remarkably adaptive and may possess advanced molecular mechanisms for host-defense against biotic and abiotic stresses [73]. Although giant African snails lack the canonical vertebrate immunoglobulin, they have developed diverse repertoires of receptors, regulators, and effectors [23]. To investigate the genes and pathways involved in immune and stress responses, we characterized the immune system on the basis of the genome of *A. immaculata*, including pattern recognition receptors, soluble factors, and mucus-related gene families (Fig. 7a, Supplementary Table 9). The transcriptomes of the hemocytes after different stimuli (lipopolysaccharide/LPS, peptidoglycan/PGN, poly (I:C)/IC and β-glucan/GLU) were also analyzed to address the potential roles of these genes (Supplementary Fig. 16).

The mucus of giant African snails is mainly composed of glycosaminoglycans

386 and glycoproteins, and its antimicrobial properties were first reported in the 1980s [74].
387 In the *A. immaculata* genome, we identified 11 heparan sulfate glucosamine
388 3-O-sulfotransferases (OSTs) functioning in glycosaminoglycan synthesis and 99
389 mucins that encode the major glycoprotein in mucus. OST genes were found to be
390 expanded in Panpulmonata (10 in *A. immaculata*, 11 in *A. fulica*, 10 in *B. glabrata*)
391 and Cephalopoda (13 in *O. bimaculoides*), in which they were two times more
392 abundant than in other mollusks (Supplementary Table 10). The expansion of OSTs in
393 Panpulmonata occurred in subfamilies OST-1 and OST-3B (Fig. 7b). Acharan sulfate,
394 a product of OST, is a primary constituent of mucus, and the expansion of the OSTs
395 was therefore closely related to the abundant surface mucus. The increased expression
396 levels of OSTs observed after LPS stimulus suggest a possible immune role in the
397 response to Gram-negative bacteria. The mucin genes were also found to be expanded
398 on the Stylommatophora branch (99 for *A. immaculate*, 71 for *A. fulica*), showing a
399 number approximately three times greater than in other mollusks, indicating that the
400 mucus of Stylommatophora contains more mucin proteins to defend against
401 microorganism infection (Supplementary Fig. 17, Supplementary Table 10). Increased
402 expression patterns of mucins were mainly detected in the LPS, IC and GLU groups,
403 implying their immune roles against Gram-negative bacteria, viruses and fungi,
404 respectively.

405 A total of 34 mucins from 19 OGs and 3 OSTs from 2 OGs were found
406 exclusively on the Stylommatophora branch (Source Data file). Their homologous
407 pseudogenes were located within the corresponding duplicated chromosomes,

indicating that these genes were generated before WGD, doubled in number through WGD, and transformed into pseudogenes after WGD (Supplementary Table 11 and 12). In addition to their roles in immunity, functions of the mucins and OSTs in wound healing, locomotion and other terrestrial-related processes were observed, indicating that their expansions before WGD may have played important roles in the A-T transition.

Discussion

WGD provides evolutionary novelties that increase environmental adaptation and species diversity, although this process is regarded as rare in animals because it is hampered by sex determination [75]. As one of the best-known simultaneous hermaphrodites [76], the giant African snail possesses the ability to undergo autofecundation under certain circumstances, thereby overcoming the evolutionary dead end resulting from WGD. Based on two high-quality assemblies from giant African snails, we report a high-credibility WGD on the Sigmurethra-Orthurethra branch (Order: Stylommatophora) with collective evidence including macrosynteny data, colinearity blocks, the gene-age distribution and Hox gene clusters. In particular, chromosome-level macrosynteny was employed for WGD identification, which was highly recommended in a recent paper to avoid possible false-positive results [17]. To the best of our knowledge, this WGD is the first to be reported in Mollusca and the first to be reported in invertebrates based on chromosome-level macrosynteny. In contrast to the two WGDs found in chelicerates (~135 and ~430 MYA), this

429 molluscan WGD was a relatively more recent event with an estimated timing of ~70
430 MYA. In contrast to ancient WGDs, the identification of this recent event will help to
431 reveal the adaptive mechanisms and consequences of WGD, especially regarding
432 subgenome divergence, providing more traceable genomic clues [77]. In most cases,
433 WGD occurs only under remarkably uncommon circumstances and provides a driving
434 force during subsequent evolution. As an example, the WGDs identified in a cluster
435 of angiosperm plants share a common causal factor corresponding with the K-T mass
436 extinction [78]. The timing of the WGD that occurred in chelicerates at ~430 MYA
437 and that in Sigmurethra-Orthurethra at~70 MYA is close to the Ordovician-Silurian
438 (O-S) extinction and the K-T mass extinction, respectively, indicating that the
439 invertebrate WGD was also connected to mass extinction events. Furthermore, it has
440 been reported that WGD is followed by a substantial increase in morphological
441 complexity and species numbers [2]. Therefore, the species richness and wide ranging
442 adaptations of invertebrates imply that more undiscovered WGDs exist in this clade
443 and might be revealed as the available genomic resources increases.

444 The A-T transition from water-living to land-living was a milestone in the
445 evolutionary history on Earth [20]. The Stylommatophora lineage, which originated
446 from a marine ancestor, and breaths through permanently air-filled lungs
447 successfully completed terrestrial adaptation approximately 100~150 MYA [79]. With
448 all the associated anatomical and physiological changes required by terrestrial living
449 [80], Stylommatophora is considered to provide good study material for the
450 investigation of the A-T transition. The WGD event and sea-level regression that

occurred during the K-T boundary are expected to have resulted in greater adaptability to terrestrial ecosystems [54]. To reveal the mechanism underlying the A-T transition and the influence of WGD, we investigated gene families related to respiration, aestivation and immune defense from the giant African snail. The terrestrial adaptation of Stylommatophora was initiated before WGD (~70 MYA), and we found that several mucus-related gene families expanded early in the Stylommatophora lineage (100~150 MYA); these genes included the mucin and OST families, functioning in water retention, immune defense and wound healing. WGD has been proposed to provide functional redundancy and mutational robustness to increase the rates of evolution and adaptation [81]. The genes encoding hemocyanins, involved in O_2 transport, and PCK and FBP, involved in gluconeogenesis, were doubled and retained after WGD, enhancing the capacity for gas exchange and glucose homeostasis in aestivation. The extra chromosome copy resulting from genome duplication might limit the risk of genetic variation in one copy of the chromosome. In the post-WGD period, zinc metalloproteinase genes were highly tandemly duplicated, resulting in the protection of tissue against ROS damage arising from respiration. This evidence indicates that although the A-T transition of the giant African snail was not initially driven by WGD, WGD could have facilitated its terrestrial adaptation by providing additional genomic resources, thus increasing the survival rate in the drastic transition from water to land.

Biological invasion has become an increasing serious problem worldwide, as the international flow of people and goods has increased over the years [82]. With its rich

473 species diversity and strong environmental adaptability, Mollusca is among the phyla
474 with the greatest numbers of invasive species, such as the golden apple snail and giant
475 African snail, which are listed among the top 100 global invasive species, although
476 the invasion mechanism of mollusks is not yet clear. Under genetic bottlenecks, the
477 invasive species can still adapt to new habitats and expand their populations, which is
478 referred to as the 'genetic paradox of invasive species' [83]. Previous reports have
479 shown that TEs are powerful facilitators of rapid adaptation that generate
480 "evolutionary potential" by introducing stress-induced changes in invasive species [84].
481 In this study, recent TE explosions were observed in all 4 invasive mollusks but were
482 absent in the other noninvasive mollusks. Genes located near recently emerged TEs
483 were enriched in the function of stress responses, which is consistent with our
484 previous findings in the golden apple snail [39], indicating that the recent TE explosion
485 might be a common genetic force contributing to biological invasion. In addition,
486 WGD has been proposed to provide robustness of genetic variation and redundant
487 gene resources for the rapid evolution of novel functions, driving phenotypic
488 complexity and ecological adaptation. Therefore, WGD may be another explanation
489 for the genetic paradox of biological invasion, and species exhibiting WGD may
490 present greater invasiveness.

491 In summary, we have revealed a WGD occurring on the Sigmurethra-Orthurethra
492 branch within Stylommatophora providing genomic evidence for the A-T transition in
493 Mollusca, and we propose WGD as a potential mechanism contributing to biological
494 invasion. In addition, the obtained genome sequences of giant African snails will

enable us to develop more environmentally friendly and efficient control measures using species-specific gene targets, benefiting the protection of agricultural crops and ecological environment as well as the prevention of human disease caused by zoonotic parasites. On the other hand, giant African snails are considered as a high-protein food source in some parts of the world, especially in Africa and Asia. The invasive characteristics of giant African snails, such as their rapid growth, high production rate, and ability to survive harsh conditions, endow them with the potential to be cultivated as an economic species. Thus, the genome sequence of giant African snails provides a powerful platform for the genetic breeding of this species, turning "waste" into wealth.

References

1 Mable, B., Alexandrou, M. & Taylor, M. Genome duplication in amphibians and fish: an extended synthesis. *Journal of Zoology* **284**, 151-182 (2011).

2 Van de Peer, Y., Maere, S. & Meyer, A. The evolutionary significance of ancient genome duplications. *Nat. Rev. Genet.* **10**, 725 (2009).

3 Clark, J. W. & Donoghue, P. C. J. Whole-genome duplication and plant macroevolution. *Trends. Plant. Sci*. **23**, 933-945 (2018).

4 Orr, H. A. " Why polyploidy is rarer in animals than in plants" revisited. *The American Naturalist* **136**, 759-770 (1990).

5 Guo, X., He, Y., Zhang, L., Lelong, C. & Jouaux, A. Immune and stress responses in oysters with insights on adaptation. *Fish Shellfish Immunol*. **46**,

107-119 (2015).

6 Hallinan, N. M. & Lindberg, D. R. Comparative analysis of chromosome counts infers three paleopolyploidies in the mollusca. *Genome. Biol. Evol.* **3**, 1150-1163 (2011).

7 Jörger, K. M. *et al.* On the origin of Acochlidia and other enigmatic euthyneuran gastropods, with implications for the systematics of Heterobranchia. *BMC Evol. Biol.* **10**, 323 (2010).

8 Cowie, R. H., Dillon, R. T., Robinson, D. G. & Smith, J. W. Alien non-marine snails and slugs of priority quarantine importance in the United States: A preliminary risk assessment. *Am. Malacol. Bull.* **27**, 113-133 (2009).

9 Comai, L. The advantages and disadvantages of being polyploid. *Nat. Rev. Genet.* **6**, 836 (2005).

10 Van de Peer, Y., Mizrachi, E. & Marchal, K. The evolutionary significance of polyploidy. *Nat. Rev. Genet.* **18**, 411 (2017).

11 Furlong, R. F. & Holland, P. W. Were vertebrates octoploid? *Philos. Trans. R. Soc. Lond. B Biol. Sci.* **357**, 531-544 (2002).

12 Hoegg, S., Brinkmann, H., Taylor, J. S. & Meyer, A. Phylogenetic timing of the fish-specific genome duplication correlates with the diversification of teleost fish. *J. Mol. Evol.* **59**, 190-203 (2004).

13 Flot, J.-F. *et al.* Genomic evidence for ameiotic evolution in the bdelloid rotifer Adineta vaga. *Nature* **500**, 453 (2013).

14 Kenny, N. J. *et al.* Ancestral whole-genome duplication in the marine

chelicerate horseshoe crabs. *Heredity* **116**, 190 (2016).

15 Schwager, E. E. *et al.* The house spider genome reveals an ancient whole-genome duplication during arachnid evolution. *BMC biol.* **15**, 62 (2017).

16 Li, Z. *et al.* Multiple large-scale gene and genome duplications during the evolution of hexapods. *PNAS* **115**, 4713-4718 (2018).

17 Nakatani, Y. & McLysaght, A. Macrosynteny analysis shows the absence of ancient whole-genome duplication in lepidopteran insects. *PNAS* **116**, 1816-1818 (2019).

18 Lillywhite, H. B., Albert, J. S., Sheehy III, C. M. & Seymour, R. S. Gravity and the evolution of cardiopulmonary morphology in snakes. *Comp. Biochem. Physiol. A Mol. Integr. Physio.* **161**, 230-242 (2012).

19 Vermeij, G. J. & Dudley, R. Why are there so few evolutionary transitions between aquatic and terrestrial ecosystems? *Biol. J. Linn. Soc.* **70**, 541-554 (2000).

20 Volkmann, D. & Baluška, F. Gravity: one of the driving forces for evolution. *Protoplasma* **229**, 143-148 (2006).

21 Little, C. *The terrestrial invasion: an ecophysiological approach to the origins of land animals*. (CUP Archive, 1990).

22 Romero, P. E., Pfenninger, M., Kano, Y. & Klussmann-Kolb, A. Molecular phylogeny of the Ellobiidae (Gastropoda: Panpulmonata) supports independent terrestrial invasions. *Mol. Phylogenet. Evol.* **97**, 43-54 (2016).

23 Mukherjee, S., Sarkar, S., Munshi, C. & Bhattacharya, S. *The Uniqueness of Achatina fulica in its Evolutionary Success*. (InTech, 2017).

24 Hiong, K. C., Loong, A. M., Chew, S. F. & Ip, Y. K. Increases in urea synthesis and the ornithine–urea cycle capacity in the Giant African Snail, Achatina fulica, during fasting or aestivation, or after the Injection with ammonium chloride. *J. Exp. Zool. A Comp. Exp. Biol.* **303**, 1040-1053 (2005).

25 Biscotti, M. A. *et al.* The Lungfish Transcriptome: A Glimpse into Molecular Evolution Events at the Transition from Water to Land. *Sci. Rep.* **6**, 21571, doi:10.1038/srep21571 (2016).

26 Bouchet, P. & Duarte, C. M. *The exploration of marine biodiversity: scientific and technological challenges*. (Fundación BBVA, 2006).

27 Thiengo, S. C., Faracas, F. A., Salgado, N. C., Cowie, R. H. & Fernandez, M. A. Rapid spread of an invasive snail in South America: the giant African snail, Achatina fulica, in Brasil. *Biol. Invasions* **9**, 693-702 (2007).

28 Ferreira, F. S., Albuquerque, U. P., Coutinho, H. D., Almeida Wde, O. & Alves, R. R. The trade in medicinal animals in northeastern Brazil. *Evid. Based Complement. Alternat. Med.* **2012**, 126938, doi:10.1155/2012/126938 (2012).

29 Serb, J. M. & Lydeard, C. Complete mtDNA sequence of the North American freshwater mussel, Lampsilis ornata (Unionidae): an examination of the evolution and phylogenetic utility of mitochondrial genome organization in Bivalvia (Mollusca). *Mol. Biol. Evol.* **20**, 1854-1866 (2003).

30 Faure, E. & Casanova, J. P. Comparison of chaetognath mitochondrial

582 genomes and phylogenetical implications. *Mitochondrion* **6**, 258-262 (2006).

583 31 Aplysia Genome Project. Broad Institute. Vertebrate Biology Group.
584 doi:https://www.broadinstitute.org/aplysia/aplysia-genome-project (2009).

585 32 Liu, B. *et al.* Estimation of genomic characteristics by analyzing k-mer
586 frequency in de novo genome projects. *arXiv* (2013). URL:
587 https://arxiv.org/abs/1308.2012.

588 33 Du, X. *et al.* The pearl oyster Pinctada fucata martensii genome and
589 multi-omic analyses provide insights into biomineralization. *Gigascience* **6**,
590 1-12 (2017).

591 34 Takeuchi, T. *et al.* Draft genome of the pearl oyster Pinctada fucata: a platform
592 for understanding bivalve biology. *DNA Res.* **19**, 117-130 (2012).

593 35 Simakov, O. *et al.* Insights into bilaterian evolution from three spiralian
594 genomes. *Nature* **493**, 526-531 (2013).

595 36 Albertin, C. B. *et al.* The octopus genome and the evolution of cephalopod
596 neural and morphological novelties. *Nature* **524**, 220-224 (2015).

597 37 Uliano-Silva, M. *et al.* A hybrid-hierarchical genome assembly strategy to
598 sequence the invasive golden mussel, Limnoperna fortunei. *Gigascience* **7**,
599 doi:10.1093/gigascience/gix128 (2018).

600 38 Adema, C. M. *et al.* Whole genome analysis of a schistosomiasis-transmitting
601 freshwater snail. *Nat. Commun.* **8**, 15451, doi:10.1038/ncomms15451 (2017).

602 39 Liu, C. *et al.* The genome of the golden apple snail Pomacea canaliculata
603 provides insight into stress tolerance and invasive adaptation. *Gigascience* **7**,

doi:10.1093/gigascience/giy101 (2018).

40 Guo, Y. *et al.* A chromosomal-level genome assembly for the giant African snail Achatina fulica. *Gigascience* **8**, doi:10.1093/gigascience/giz124 (2019).

41 Tan, S. K. & Low, M. E. Y. An update to the West African Limicolaria flammea (Müller, 1774) in Singapore, and its distinction from the confamilial Achatina fulica Bowdich, 1822 (Mollusca: Gastropoda: Achatinidae). *Nature in Singapore* **4**, 311-317 (2011).

42 Koren, S. *et al.* Canu: scalable and accurate long-read assembly via adaptive k-mer weighting and repeat separation. *Genome Res.* **27**, 722-736 (2017).

43 Ruan, J. & Li, H. Fast and accurate long-read assembly with wtdbg2. *BioRxiv*, (2019). URL: https://www.biorxiv.org/content/10.1101/530972v1.full. DOI: https://doi.org/10.1101/530972.

44 Walker, B. J. *et al.* Pilon: an integrated tool for comprehensive microbial variant detection and genome assembly improvement. *PloS one* **9**, e112963 (2014).

45 Stamatakis, A. RAxML version 8: a tool for phylogenetic analysis and post-analysis of large phylogenies. *Bioinformatics* **30**, 1312-1313 (2014).

46 Sanderson, M. J. r8s: inferring absolute rates of molecular evolution and divergence times in the absence of a molecular clock. *Bioinformatics* **19**, 301-302 (2003).

47 Feschotte, C. & Wessler, S. R. Mariner-like transposases are widespread and diverse in flowering plants. *Proceedings of the National Academy of Sciences*

99, 280-285 (2002).

48 Hua-Van, A., Le Rouzic, A., Boutin, T. S., Filée, J. & Capy, P. The struggle for life of the genome's selfish architects. *Biology direct* **6**, 19 (2011).

49 Werren, J. H. Selfish genetic elements, genetic conflict, and evolutionary innovation. *PNAS* **108**, 10863-10870 (2011).

50 Amores, A. *et al.* Zebrafish hox clusters and vertebrate genome evolution. *Science* **282**, 1711-1714 (1998).

51 Sessa, E. B. Polyploidy as a mechanism for surviving global change. *New Phytol.* **221**, 5-6 (2019).

52 Petersen, S. V., Dutton, A. & Lohmann, K. C. End-Cretaceous extinction in Antarctica linked to both Deccan volcanism and meteorite impact via climate change. *Nat. Commun.* **7**, 12079 (2016).

53 Fawcett, J. A., Maere, S. & Van De Peer, Y. Plants with double genomes might have had a better chance to survive the Cretaceous–Tertiary extinction event. *PNAS* **106**, 5737-5742 (2009).

54 Marshall, C. R. & Ward, P. D. Sudden and gradual molluscan extinctions in the latest Cretaceous of western European Tethys. *Science* **274**, 1360-1363 (1996).

55 Thiriot-Quiévreux, C. Advances in chromosomal studies of gastropod molluscs. *J. Mollus. Stud.* **69**, 187-202 (2003).

56 Aktipis, S. W. & Giribet, G. A phylogeny of Vetigastropoda and other “archaeogastropods”: re-organizing old gastropod clades. *Invertebr. Biol.* **129**,

220-240 (2010).

57 Ashley-Ross, M. A., Hsieh, S. T., Gibb, A. C. & Blob, R. W. Vertebrate land invasions-past, present, and future: an introduction to the symposium. *Integr. Comp. Biol.* **53**, 192-196 (2013).

58 Hsia, C. C., Schmitz, A., Lambertz, M., Perry, S. F. & Maina, J. N. Evolution of air breathing: oxygen homeostasis and the transitions from water to land and sky. *Compr. Physiol.* **3**, 849-915 (2013).

59 Markl, J. Evolution of molluscan hemocyanin structures. *Biochim. Biophys. Acta* **1834**, 1840-1852 (2013).

60 Kato, S., Matsui, T., Gatsogiannis, C. & Tanaka, Y. Molluscan hemocyanin: structure, evolution, and physiology. *Biophys. Rev.* **10**, 191-202 (2018).

61 Shen, S. *et al.* ABCG2 reduces ROS-mediated toxicity and inflammation: a potential role in Alzheimer's disease. *J. Neurochem.* **114**, 1590-1604 (2010).

62 Kruse, M. N. *et al.* Human meprin α and β homo-oligomers: cleavage of basement membrane proteins and sensitivity to metalloprotease inhibitors. *Biochem. J.* **378**, 383–389 (2004).

63 Faa, G. *et al.* Zinc in gastrointestinal and liver disease. *Coordin. Chem. Rev.* **252**, 1257-1269 (2008).

64 Storey, K. B. Life in the slow lane: Molecular mechanisms of estivation. *Comp. Biochem. Physiol. A Mol. Integr. Physiol.* **133**, 733-754 (2002).

65 Ip, Y. K. & Chew, S. F. *Nitrogen Metabolism and Excretion During Aestivation*. (Springer Heidelberg Dordrecht London New York, 2010).

66 Bell, R. A., Dawson, N. J. & Storey, K. B. Insights into the in vivo regulation of glutamate dehydrogenase from the foot muscle of an estivating land snail. *Enzyme Res*. **2012**, 317314, doi:10.1155/2012/317314 (2012).

67 Bulutoglu, B., Garcia, K. E., Wu, F., Minteer, S. D. & Banta, S. Direct Evidence for Metabolon Formation and Substrate Channeling in Recombinant TCA Cycle Enzymes. *ACS Chem. Biol.* **11**, 2847-2853 (2016).

68 Oja, S. S., Saransaari, P. & Korpi, E.R. Neurotoxicity of Ammonia. *Neurochem. Res*. **42**, 713 (2017).

69 Hermenegildo, C., Monfort, P. & Felipo, V. Activation of N-Methyl-D-Aspartate Receptors in Rat Brain In Vivo Following Acute Ammonia Intoxication: Characterization by In Vivo Brain Microdialysis. *Hepatology* **31**, 709-715 (2000).

70 Onadeko, A. B. & Egonmwan, R. I. Water Relations, Weight Loss and Nitrogenous Waste Products in the Giant African Land Snail Archachatina Marginata (Swainson) – Pulmonata: Achatinidae. *J. Sci. Res. Dev.* **17**, 40-47 (2017).

71 Diez-Fernandez, C., Gallego, J., Haberle, J., Cervera, J. & Rubio, V. The Study of Carbamoyl Phosphate Synthetase 1 Deficiency Sheds Light on the Mechanism for Switching On/Off the Urea Cycle. *J Genet Genomics* **42**, 249-260 (2015).

72 Wang, L., Qiu, L., Zhou, Z. & Song, L. Research progress on the mollusc immunity in China. *Dev. Comp. Immunol.* **39**, 2-10 (2013).

73 Begum, N., Matsumoto, M., Tsuji, S., Toyoshima, K. & Seya, T. The primary host defense system across humans, flies and plants. *Curr. Trends Immunol.* **3**, 59-74 (2000).

74 Iguchi, S. M., Aikawa, T. & Matsumoto, J. J. Antibacterial activity of snail mucus mucin. *Comp. Biochem. Physiol. A Physio.* **72**, 571-574 (1982).

75 Wertheim, B., Beukeboom, L. & Van de Zande, L. Polyploidy in animals: effects of gene expression on sex determination, evolution and ecology. *Cytogenet. Genome Res.* **140**, 256-269 (2013).

76 Barrows, E. M. *Animal behavior desk reference: a dictionary of animal behavior, ecology, and evolution*. (CRC press, 2000).

77 Soltis, D. E. *et al.* Polyploidy and angiosperm diversification. *Am. J. Bot.* **96**, 336-348 (2009).

78 Vanneste, K., Baele, G., Maere, S. & Van de Peer, Y. Analysis of 41 plant genomes supports a wave of successful genome duplications in association with the Cretaceous–Paleogene boundary. *Genome Res.* **24**, 1334-1347 (2014).

79 Kameda, Y. & Kato, M. Terrestrial invasion of pomatiopsid gastropods in the heavy-snow region of the Japanese Archipelago. *BMC Evol. Biol.* **11**, 118 (2011).

80 Barker, G. M. *Gastropods on land: phylogeny, diversity and adaptive morphology*. 1-146 (CAB International, 2001).

81 Crow, K. D. & Wagner, G. P. What is the role of genome duplication in the evolution of complexity and diversity? *Mol. Biol. Evol.* **23**, 887-892 (2006).

82 Wan, F., Jiang, M. & Zhan, A. *Biological invasions and its management in china*. Vol. 1 (Springer, 2017).

83 Frankham, R. Resolving the genetic paradox in invasive species. *Heredity* **94**, 385-385 (2005).

84 Stapley, J., Santure, A. W. & Dennis, S. R. Transposable elements as agents of rapid adaptation may explain the genetic paradox of invasive species. *Mol. Ecol*. **24**, 2241-2252 (2015).

Figure legends

Figure 1. The general characteristics of *A.immaculata*. (a) The morphological difference: *A. immaculata* has relatively longer shell with pink or purple columella, while *A. fulica* has shorter shell with white columella. (**b**) Global invasion regions for *A. immaculata* (top) and *A. fulica* (bottom). Currently, *A. fulica* is more widely distributed, but *A. immaculata* has more advantage with a faster invasion speed. **(c)** The sketch map showed the major physiological specialty of *A. immaculata*, including immune innovation, eupulmonates lung, estivation and mucus. **(d)** Genomic features showed by Circos plot**.** Track n: 31 linkage groups of the genome; Track d-m: expression profile of brain, egg, eye, hemocytes, hepatopancreas, kidney, lungs, muscle, ovary and testis tissues; Track c: distribution of transposon elements; Track b:

735 distribution of gene density; Track a: distribution of GC content.

736 **Figure 2. Evolutionary analysis of *A.immaculata*. (a)** Phylogenetic placement of *A.*
737 *immaculata* within the dated tree of mollusks. The estimated divergence time is
738 shown at each branching point, and each lineage is shown in different color blocks. *A.*
739 *immaculata* is highlighted in red. **(b)** Categories of orthologous and paralogous genes
740 in various phyla and species. **(c)** Classification and contents of repetitive sequences in
741 *A. immaculata* and other mollusks. **(d)** Distribution of divergence rate for the class of
742 DNA transposons in mollusks genomes. The divergence rate was calculated by
743 comparing all TE sequences identified in the genome to the corresponding consensus
744 sequence in each TE subfamily. The arrow indicates that both *A. immaculata* and *A.*
745 *fulica* had a recent explosion of TEs at divergence rate of ~5%.

746 **Figure 3. Whole genome duplication shared by *A. immaculata* and *A. fulica*.**
747 Circos plots showed the homologous gene pairs in chromosome-level microsynteny
748 among the *A. immaculata* **(a)** and *A. fulica* **(b)** individually, as well as chromosomes
749 between *A. immaculata* and *A. fulica* **(c),** *A. immaculata* and *P. canaliculata* **(d)**, *A.*
750 *immaculata* and *P. fucata* **(e)**. **(f)** Gene age distribution of Ks values calculated from
751 orthologous gene pairs, among *A. immaculata, A. fulica, and P. canaliculata*
752 individually, as well as between *A. immaculata and A. fulica*, *A. immaculata and B.*
753 *glabrata.* **(E)** Comparison of the catalog of Hox genes. *A. immaculata* and *A. fulica*
754 have more Hox genes than the other molloscus, because of the retained genes on the
755 duplicated chromosome. These evidences collectively support a whole genome

duplication event shared by *A. immaculata and A. fulica*, which is not found in other mollusks.

Figure 4. Chromosome relationship and karyotype inferring. Clustering of chromosomes for *A. immaculata* **(a)** and *A. fulica* **(b)**. Each group corresponding to an orthologous chromosome pair derived from WGD, with the links between chromosome pairs representing the mutual best-hit gene pairs. **(c)** Evolution of karyotype in mollusks. The common ancestor of Gastropoda and Bivalvia is estimated to have 8 monoploid chromosomes, while that of Gastropoda has 14. Chromosome breaks, fusions, as well as chromosome number doubling by WGD, formed the current karyotype of living mollusks.

Figure 5. Oxygen transport and anti-oxidization in the respiratory. **(a)** The phylogenetic relationship of hemocyanin genes among mollusks. The protein IDs covered with different colors meant different species. (**b**) The phylogenetic relationship of zinc metalloproteinases among gastropoda, with same style to that of (**a**). (**c**) Comparison of hemocyanin locations in the chromosomes of *A. immaculata*, *A. fulica* and *P. canaliculata*. Hemocyanin genes of *A. immaculata* and *A. fulica* were distributed in two chromosomes, whereas *P. canaliculata* was only in one contig. (**d**) The evolution process of zinc metalloproteinase genes in *A. immaculata* and *A. fulica*. The shared ancient ancestor might have only one zinc metalloproteinase gene located on one chromosome, WGD (~70 MYA) event doubles the chromosome and gene number, followed by gene expansion on one chromosome and deletion on the corresponding chromosome, resulting in a tandem-cluster of 11 genes and 9 genes in

A. immaculata and *A. fulica*, respectively.

Figure 6. Flowchart of glucose homeostasis and urea-cycle in aestivation of *A. immaculata*. (**a**)The key processes and related gene expression change of gluconeogenesis and TCA cycle in aestivation compared with normal group. The left part represented the major genes participated in gluconeogenesis, while the right part represented the major genes participated in TCA cycle. Two types of arrows were used, double-line arrow meant a number of steps, and single-line arrow meant one step. Two shapes were used, rectangle meant production, and ellipse meant enzymes, with color red and blue representing up-regulated and down-regulated respectively. Ellipse with symbol "*" meant this enzyme had two genes derived from WGD. (**b**) The key processes and related gene expression change of ornithine-urea cycle in aestivation compared with normal groups, the style is same to that of (**a**).

Figure 7. The immune repertoire of *A. immaculata* and the expansion of OST. (a) The immunity of *A. immaculata* is presented in mucus, pattern recognition receptors, and soluble effectors. The mucus system covered epidermis, mainly including archacin, mucin and acharan sulfate secreted through the NDST pathway, which were presented with green ellipse. The pattern recognition system on the cytomembrane (orange color) contained PGRP, lectin, TFNR, TLR, FREP, GNBP, SR, TEP, and secreted soluble effector (red ellipse) in the downstream immune cascading. (**b**) The expansion of OST genes. Phylogenetic analyses were performed using MEGA7 through maximum likelihood. The OST genes from different species were indicated in circus filled with different colors.

Methods

Samples collection and genome sequencing

Adults of *A. immaculata* were collected from a local farm in Yangjiang, Guangdong province, China, and maintained at 25 ± 2 °C for a week before processing. Genomic DNA was extracted from the foot muscles of a single snail for constructing PCR-free Illumina 350-bp insert libraries and PacBio 20-kb insert library, and sequenced on Illumina HiSeq-X and PacBio SMRT platforms, respectively. The Hi-C library was prepared using the muscle tissue of another single snail by the following methods: Nuclear DNA was cross-linked in situ, extracted, and then digested with a restriction enzyme. The sticky ends of the digested fragments were biotinylated, diluted, and then ligated to each other randomly. Biotinylated DNA fragments were enriched and sheared again for preparing the sequencing library, which was then sequenced on a HiSeq-X platform (Illumina).

RNA sample preparation and transcriptome sequencing

Ten tissues including brains, eggs (2 days post fertilization), eyes, hemocytes, hepatopancreas, kidneys, lungs, muscles, ovaries and testes from six animals were collected as replicates. Eighty snails were employed for the immune elicitor challenge experiment, and they were equally divided into control group, LPS (lipopolysaccharide) group, PGN (peptidoglycan) group, GLU (β-glucan) group and IC (poly I:C) group. The five groups of snails received injections of 100 μL

phosphatic buffer solution (PBS, 0.14 M NaCl, 3 mM KCl, 8 mM $NaH_2PO_4 \cdot 12H_2O$, 1.5 mM K_2HPO_4, pH7.4), LPS from *Escherichia coli* 0111:B4 (Sigma-Aldrich, 0.5 $mg \cdot ml^{-1}$ in PBS), PGN from *Staphylococcus aureus* (Sigma-Aldrich, 0.8 $mg \cdot ml^{-1}$ in PBS), GLU from *Saccharomyces cerevisiae* (Sigma-Aldrich, 1.0 $mg \cdot ml^{-1}$ in PBS), and poly I:C (Sigma-Aldrich, 1.0 $mg \cdot ml^{-1}$ in PBS), respectively. These treated snails were maintained after injection, and fifteen individuals from each group were randomly sampled at 12 h post-injection. Non-aestivation snails were feeding with enough food and water, whereas aestivation snails were fasting and treated with high temperature, and hemolymph of these two groups were collected around 10 days after the epiphragma formation. Hemolymph samples of all the treated group were collected from five individuals were pooled into one sample. There were three replicates for each sample. In final, total RNAs were extracted from the stored tissues, and then mRNAs were pulled out by beads with poly-T for constructing cDNA libraries (insert 350-bp), and sequenced on an Illumina HiSeq-X sequencer.

Genome assembly

The Illumina raw reads were filtered by trimming the adapter sequence and low-quality regions (https://github.com/fanagislab/assembly_2ndGeneration/tree/master/clean_illumina), resulting in clean and high-quality reads with an average error rate < 0.001. For the PacBio raw data, the short subreads (< 2 kb) and low-quality (error rate > 0.2) subreads were filtered out, and only one representative subread was retained for each

PacBio read. The clean PacBio reads were corrected by Canu 1.8 [42] and then assembled by Wtdbg2 [43]. The PacBio reads were employed to polish the raw contigs by a module within Wtdbg2, after which Illumina reads were aligned to the contigs by BWA-MEM, and single base errors in the contigs were corrected by Pilon 2.10 [44] with the parameters "-fix bases, -nonpf, -minqual 20". Next, Hi-C sequencing data were aligned to the haploid reference contigs by HiC-Pro 2.11.1 [85], and then these contigs were clustered, ordered, and orientated into chromosomes with LACH-ESIS [86].

Genome annotation

A de novo repeat library for *A. immaculata* was constructed by RepeatModeler (v1.0.4; http://www.repeatmasker.org/RepeatModeler.html). TEs in the *A. immaculata* genome were identified by RepeatMasker (v4.0.6; http://www.repeatmasker.org/) using both the Repbase library and the de novo library. Tandem repeats in the *A. immaculata* genome were predicted using Tandem Repeats Finder v4.07b [87]. The divergence rates of TEs were calculated between the identified TE elements in the genome and their consensus sequence at the TE family level.

The gene models in the *A. immaculata* genome were predicted by EVM v1.1.1 [88] integrating evidences from ab initio predictions, homology-based searches and RNA-seq alignments. Then, these gene models were annotated by RNA-seq data, UniProt database and InterProScan software [89]. Finally, the gene models were retained if they had at least one piece of supporting evidence from the UniProt database, InterProScan domain and RNA-seq data. Gene functional annotation was performed

by aligning the protein sequences to the NCBI NR, UniProt, COG and KEGG databases with BLASTP v2.3.0+ under an E-value cutoff of 10^{-5} and choosing the best hit. Pathway analysis and functional classification were conducted based on the KEGG database [90]. InterProScan was used to assign IPR domains and GO terms to the gene models.

Evolutionary analysis

Orthologous and paralogous groups were assigned from 11 species (*A. immaculata, A. fulica, Aplysia californica, Biomphalaria glabrata, Pomacea canaliculata, Lottia giganta, Crassostrea gigas, Pintada fucata, Limnoperna fortune, Octopus bimaculoide* and *Lingula anatina*) by OrthoFinder [91] with default parameters. OGs that contained only one gene for each species were selected to construct the phylogenetic tree. The protein sequences of each gene family were independently aligned by muscle v3.8.31 [92] and then concatenated into one super-sequence. The phylogenetic tree was constructed by maximum likelihood (ML) using RAxML 8.2.12 [45], with the best-fit model (LG+IGF) estimated by ProtTest3 [93]. The absolute rates of molecular evolution and divergence times were estimated by r8s [46]. The tree was calibrated with the following time frames to constrain the age of the nodes between the species: minimum = 260 Ma and maximum = 290 MYA for *P. fucata* and *C. gigas* [94]; minimum = 450 MYA and maximum = 480 MYA for *A. californica* (or *B. glabrata*) and *L. giganta* [95]. The calibration time (fossil record time) interval (550-610 MYA) of *O. bimaculoides* was adopted from previous results [96].

Transcriptome data analysis

Transcriptome reads were trimmed with the same method for genomic reads (https://github.com/fanagislab/assembly_2ndGeneration/tree/master/clean_illumina), and then mapped to the reference genome of *A. immaculata* using TopHat (v. 2.1.0) with default settings. The expression level of each reference gene in terms of FPKM was computed by cufflinks v2.2.1. A gene was considered to be expressed if the FPKM > 0. Differential gene expression analysis was conducted using cuffdiff v2.2.1.

WGD verification

The analyses incorporating chromosome-level macrosynteny analysis, colinearity blocks, Ks peak and Hox gene clusters were employed to verify the WGD in giant African snails. Based on 4 chromosome-level molluscan genomes, the macrosynteny was identified using homologous gene sets. Genes from different species would be identified as homologous gene pairs when they had mutual best BLASTP hits with each other. The conserved macrosynteny between species with chromosome-level assemblies was displayed in dot plot. Each dot in the dot plot comparison represents a one-to-one homologous gene pair mentioned above. Based on the dot plot, we inferred the circus plot and dual synteny plot. Then, MCScanX was also used with default parameters to identify the colinearity blocks in *A. immaculata* and *A. fulica* [97]. Ks distribution of gene pairs in colinearity blocks was calculated by ParaAT [98] and KaKs_calculator 2.0 [99]. The homeobox genes were identified in the giant African snails using BLAST ($E < e^{-5}$) against all homeodomain sequences from the

HomeoDB database (http://homeodb.zoo.ox.ac.uk/), and were further confirmed by comparing to the Conserved Domains Database (http://www.ncbi.nlm.nih.gov/cdd).

Gene family analysis

To identify gene families involved in pathways of respiration, aestivation and immune functions, we performed manual curation for identification of homologous genes by three steps. Initially, we aligned known genes of other close species to the *A. immaculata* genome by BLASTP with best hits ($E < e^{-5}$), and followed by the analysis of paralogous genes performed by OrthoFinder. Then, the obtained genes were used to perform phylogeny analysis by maximum likelihood (ML) method with MEGA7 [100], to further validate the accuracy and reveal the phylogenetic relationship of these genes.

Data availability

Data relating with the findings of this work are available within the paper and the Supplementary Information files. A reporting summary for this Article is available as a Supplementary Information file. Source data are provided as a Source Data file. All the raw sequencing data generated during this study have been deposited at NCBI as a BioProject under accession PRJNA561271. Genomic and transcriptome sequence reads have been deposited in the SRA database with BioSample: SAMN12612888. The Whole Genome Shotgun project of A. immaculata has been deposited at DDBJ/ENA/GenBank under the accession WNKJ00000000. The version described in

this paper is version WNKJ00000000. The genome assemblies and annotation files are available at the website ftp://ftp.agis.org.cn/~fanwei/Achatina_immaculata_genome/.

Code availability

The in-house software clean_adapter [https://github.com/fanagislab/assembly_2ndGeneration/blob/master/clean_illumina/clean_adapter] and clean_lowqual [https://github.com/fanagislab/assembly_2ndGeneration/blob/master/clean_illumina/clean_lowqual] are used to filter the adapter and low-quality sequence.

Methods references

85 Servant, N. *et al.* HiC-Pro: an optimized and flexible pipeline for Hi-C data processing. *Genome Biol.* **16**, 259 (2015).

86 Burton, J. N. *et al.* Chromosome-scale scaffolding of de novo genome assemblies based on chromatin interactions. *Nat. Biotechnol.* **31**, 1119 (2013).

87 Benson, G. Tandem repeats finder: a program to analyze DNA sequences. *Nucleic Acids Res.* **27**, 573-580 (1999).

88 Haas, B. J. *et al.* Automated eukaryotic gene structure annotation using EVidenceModeler and the Program to Assemble Spliced Alignments. *Genome Biol.* **9**, R7, doi:10.1186/gb-2008-9-1-r7 (2008).

89 Jones, P. *et al.* InterProScan 5: genome-scale protein function classification.

Bioinformatics **30**, 1236-1240 (2014).

90 Aoki, K. F. & Kanehisa, M. Using the KEGG database resource. *Current protocols in bioinformatics* **11**, 1.12. 11-11.12. 54 (2005).

91 Emms, D. M. & Kelly, S. OrthoFinder: solving fundamental biases in whole genome comparisons dramatically improves orthogroup inference accuracy. *Genome Biol.* **16**, 157 (2015).

92 Edgar, R. C. MUSCLE: multiple sequence alignment with high accuracy and high throughput. *Nucleic Acids Res.* **32**, 1792-1797 (2004).

93 Darriba, D., Taboada, G. L., Doallo, R. & Posada, D. ProtTest 3: fast selection of best-fit models of protein evolution. *Bioinformatics* **27**, 1164-1165 (2011).

94 Sun, J. *et al.* Adaptation to deep-sea chemosynthetic environments as revealed by mussel genomes. *Nat. Ecol. Evol.* **1**, 0121 (2017).

95 Benton, M., Donoghue, P. & Asher, R. *The Timetree of Life, chapter Calibrating and constraining molecular clocks*. (Oxford University Press, 2009).

96 Zapata, F. *et al.* Phylogenomic analyses of deep gastropod relationships reject Orthogastropoda. *P. Roy. Soc. B Biol. Sci* **281**, 20141739 (2014).

97 Wang, Y. *et al.* MCScanX: a toolkit for detection and evolutionary analysis of gene synteny and collinearity. *Nucleic Acids Res.* **40**, e49-e49 (2012).

98 Zhang, Z. *et al.* ParaAT: a parallel tool for constructing multiple protein-coding DNA alignments. *Biochem. Biophys. Res. Commun.* **419**, 779-781 (2012).

99 Wang, D., Zhang, Y., Zhang, Z., Zhu, J. & Yu, J. KaKs_Calculator 2.0: a toolkit incorporating gamma-series methods and sliding window strategies. *Genom. Proteom. Bioinf.* **8** 77-80 (2010).

100 Kumar, S., Stecher, G. & Tamura, K. MEGA7: Molecular Evolutionary Genetics Analysis Version 7.0 for Bigger Datasets. *Mol. Biol. Evol.* **33**, 1870-1874 (2016).

Acknowledgements

The work was funded by the National key research and development program of China (2016YFC1200600), the Agricultural Science and Technology Innovation Program && The Elite Young Scientists Program of CAAS, Fundamental Research Funds for Central Non-profit Scientific Institution (No.Y2017JC01), the Agricultural Science and Technology Innovation Program Cooperation and Innovation Mission (CAAS-XTCX2016), Fund of Key Laboratory of Shenzhen (ZDSYS20141118170111640), as well as National Natural Science Foundation of China (Grant Nos. 31801804).

Author contributions

W. F. and W. Q. Q. conceived and led the project; C. H. L. and Y. W. R. prepared DNA and RNA for sequencing; C. H. L. performed genome assembly, annotation, evolution, whole genome duplication, and immune analysis; Y.W.R. performed

respiration and aestivation analysis; W. F., W. Q. Q., C. H. L. and Y. W. R. wrote and revised the manuscript.

Competing interests

The authors declare no competing interests.

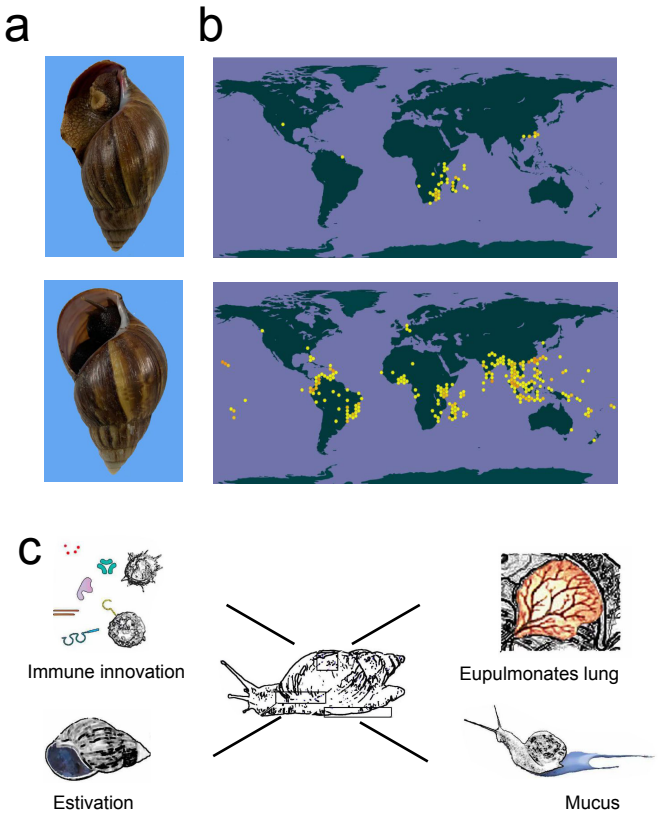

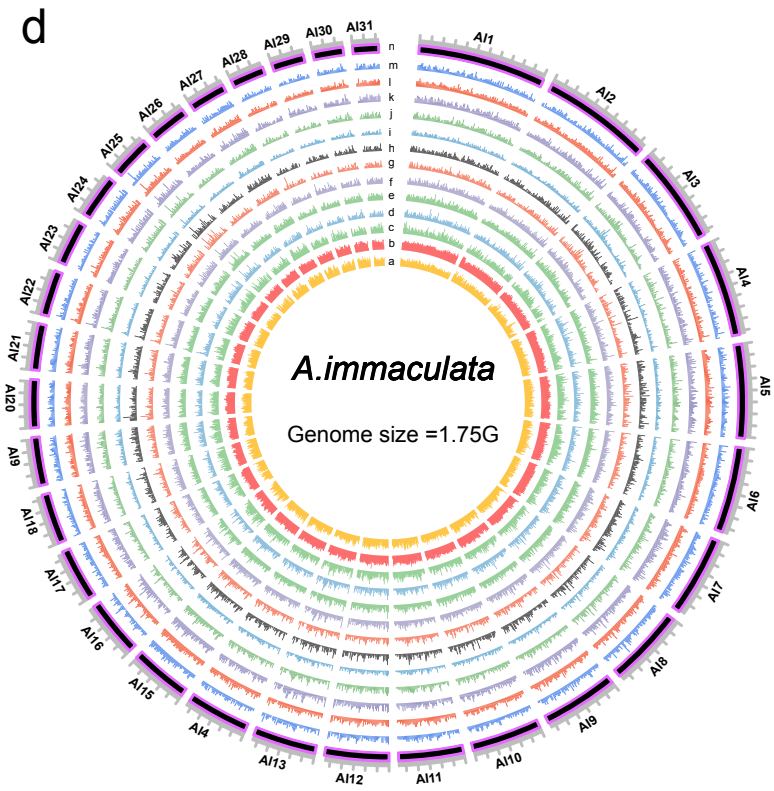

a

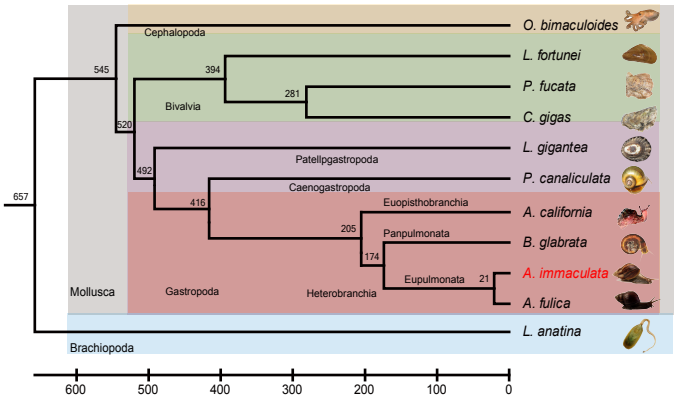

b

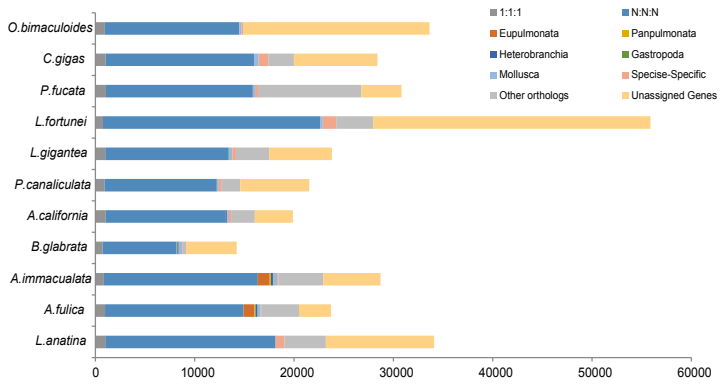

c

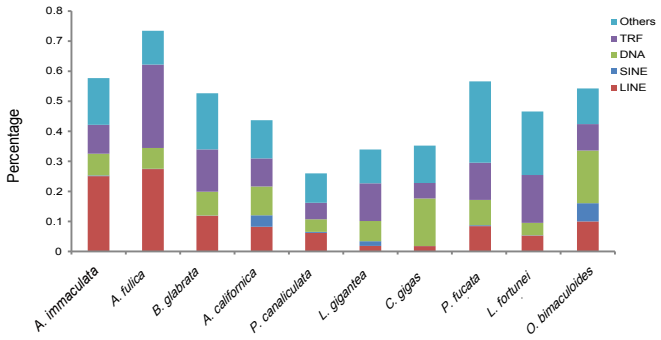

d

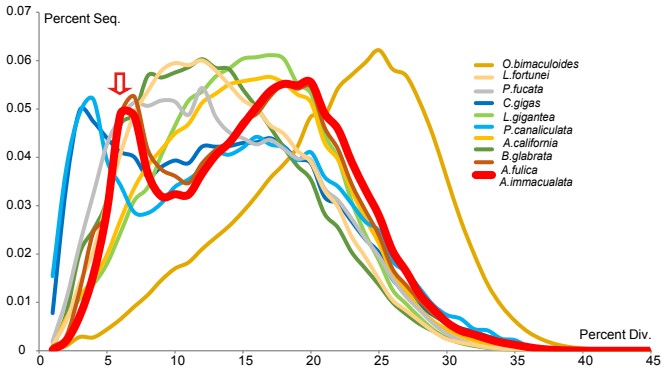

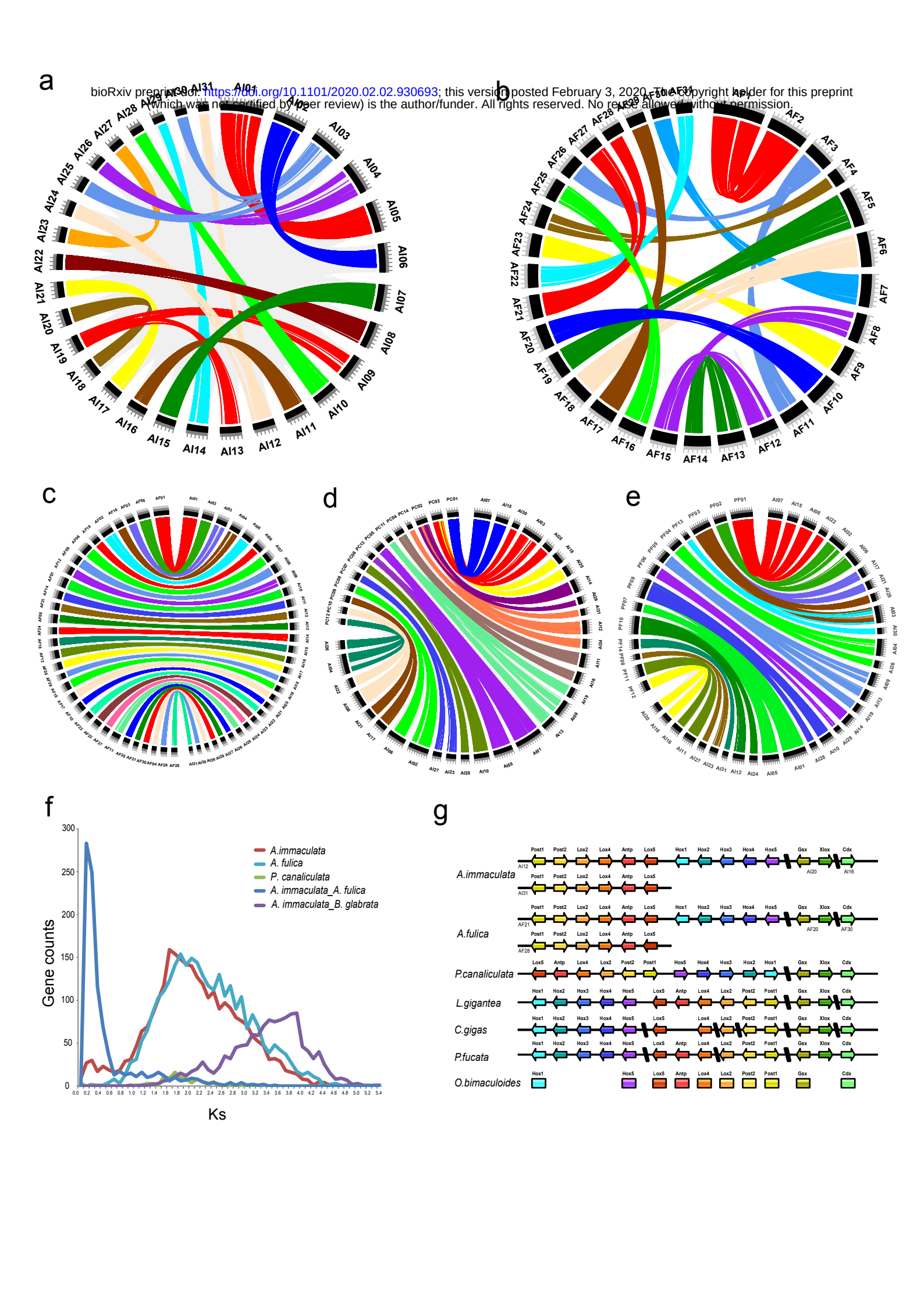

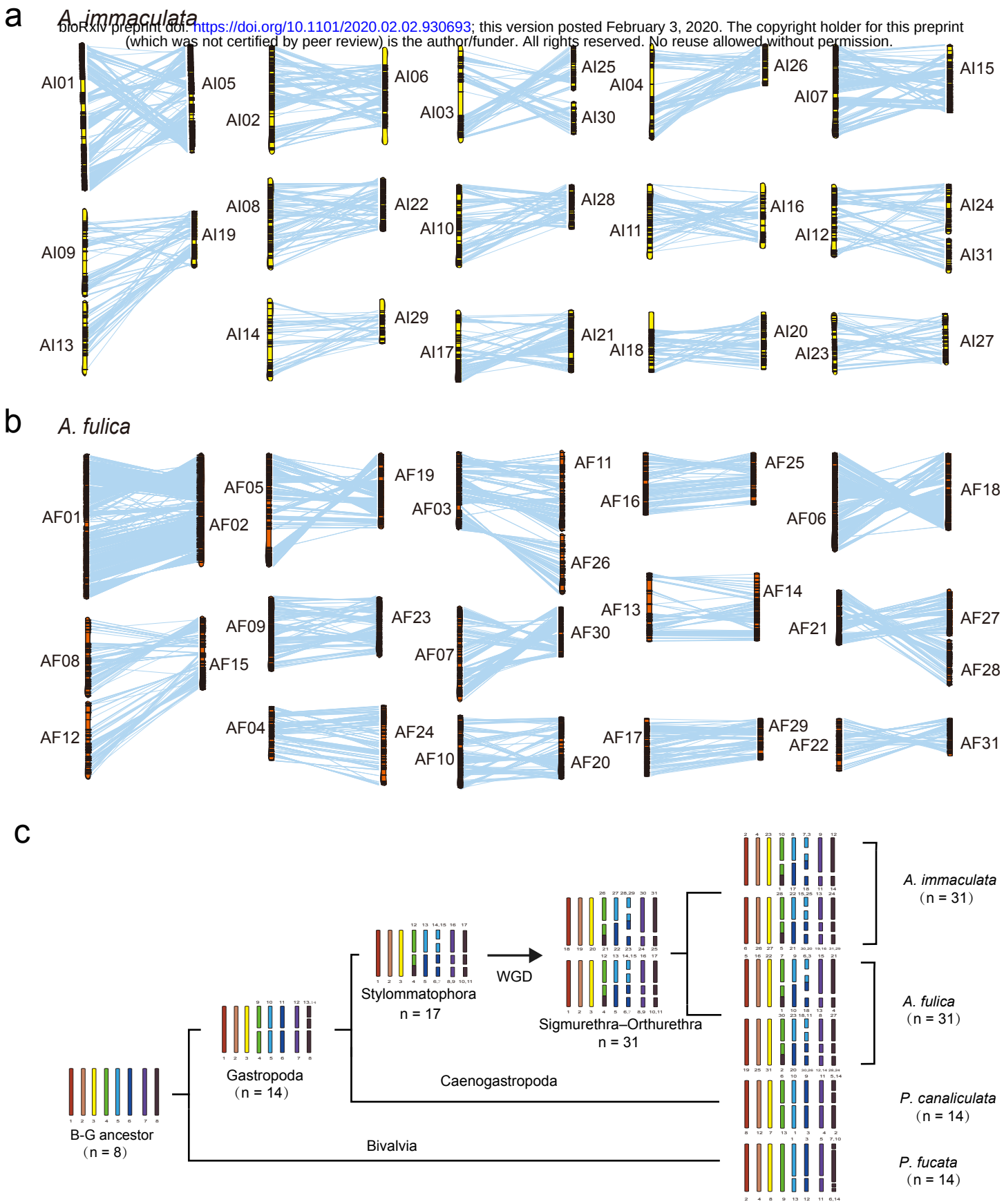

a

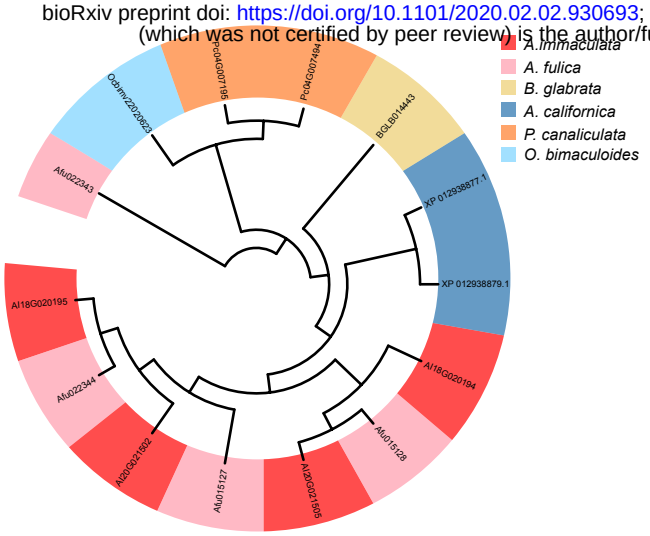

b

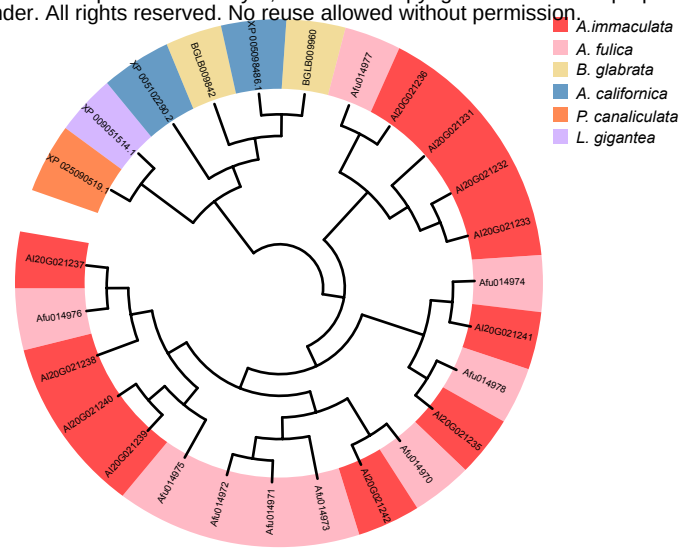

c

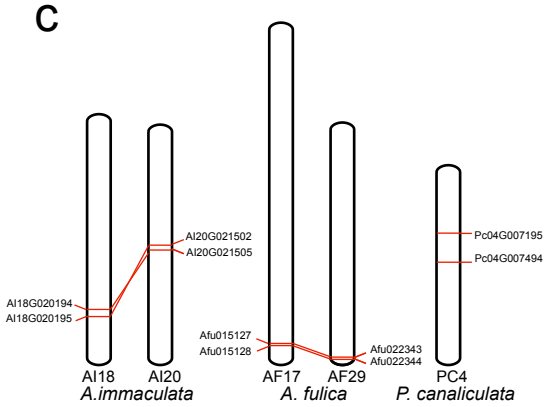

d

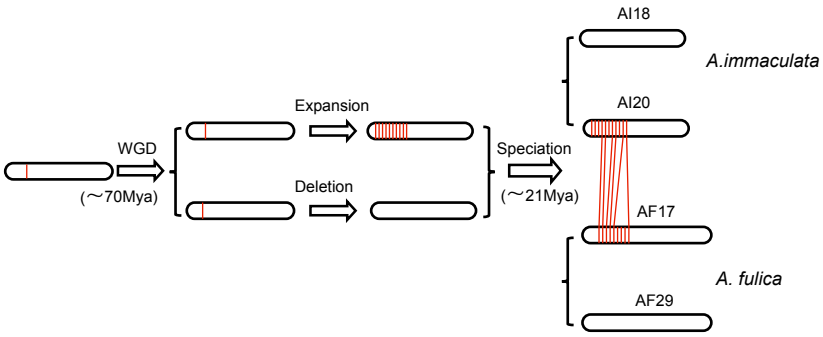

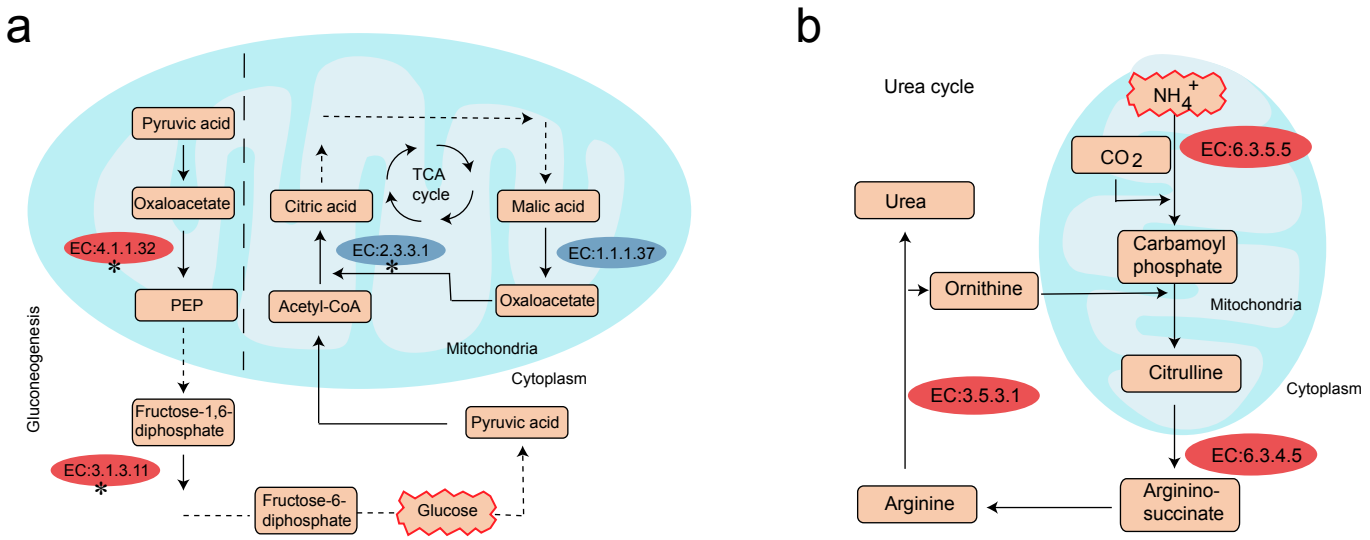

a

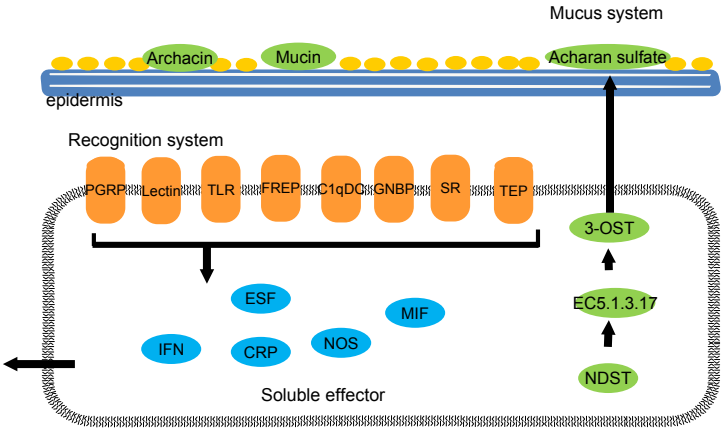

b